

Isolated corona current monitoring using a compensated light-emitting diode as an unpowered sensor

Article

Published Version

Creative Commons: Attribution 4.0 (CC-BY)

Open Access

Harrison, R. G. ORCID: <https://orcid.org/0000-0003-0693-347X>, Escobar Ruiz, V. ORCID: <https://orcid.org/0000-0003-1336-0921>, Nicoll, K. ORCID: <https://orcid.org/0000-0001-5580-6325> and Ambaum, M. H. P. ORCID: <https://orcid.org/0000-0002-6824-8083> (2023) Isolated corona current monitoring using a compensated light-emitting diode as an unpowered sensor. *Review of Scientific Instruments*, 94 (9). 094504. ISSN 1089-7623 doi: 10.1063/5.0170176 Available at <https://centaur.reading.ac.uk/113201/>

It is advisable to refer to the publisher's version if you intend to cite from the work. See [Guidance on citing](#).

To link to this article DOI: <http://dx.doi.org/10.1063/5.0170176>

Publisher: AIP

All outputs in CentAUR are protected by Intellectual Property Rights law, including copyright law. Copyright and IPR is retained by the creators or other copyright holders. Terms and conditions for use of this material are defined in the [End User Agreement](#).

www.reading.ac.uk/centaur

CentAUR

Central Archive at the University of Reading

Reading's research outputs online

RESEARCH ARTICLE | SEPTEMBER 22 2023

Isolated corona current monitoring using a compensated light-emitting diode as an unpowered sensor

R. Giles Harrison  ; Veronica Escobar-Ruiz  ; Keri A. Nicoll  ; Maarten H. P. Ambaum 



Rev. Sci. Instrum. 94, 094504 (2023)

<https://doi.org/10.1063/5.0170176>



Export
Citation

CrossMark

Articles You May Be Interested In

Research on pressure fluctuation induced by tip leakage vortex of axial flow circulating pump under unpowered driven conditions



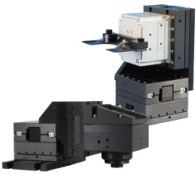
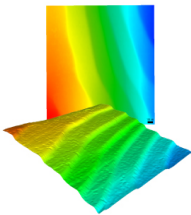
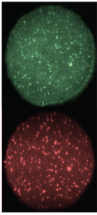
Physics of Fluids (March 2023)

Refractive index gradients and light scattering in polymer-dispersed liquid crystal films

Appl. Phys. Lett. (March 1993)

Microstructural evolution and atomic transport by thermomigration in eutectic tin-lead flip chip solder joints

J. Appl. Phys. (August 2007)

 MCL MAD CITY LABS INC. www.madcitylabs.com	<p>Nanopositioning Systems</p> 	<p>Modular Motion Control</p> 	<p>AFM and NSOM Instruments</p> 	<p>Single Molecule Microscopes</p> 
---	--	--	---	--

Isolated corona current monitoring using a compensated light-emitting diode as an unpowered sensor

Cite as: Rev. Sci. Instrum. 94, 094504 (2023); doi: 10.1063/5.0170176

Submitted: 1 August 2023 • Accepted: 2 September 2023 •

Published Online: 22 September 2023



R. Giles Harrison,^{a)} Veronica Escobar-Ruiz, Keri A. Nicoll, and Maarten H. P. Ambaum

AFFILIATIONS

Department of Meteorology, University of Reading, Reading RG6 6ET, United Kingdom

^{a)} Author to whom correspondence should be addressed: r.g.harrison@reading.ac.uk

ABSTRACT

Measurement of the emission current at a high voltage is necessary in monitoring ion production from a corona source, to provide independent confirmation of operation. The wide common mode range required is usually obtained through an isolated system, which requires isolated power to operate, adding complexity and volume. Passing the current through a light-emitting diode (LED) provides an alternative measurement method as the LED's brightness can be used to signal the current's magnitude. The forward voltage loss across the LED is negligible compared with the emitter voltage. Selection of a discrete LED for this task rather than using one within a standard integrated optocoupler package improves the low current sensitivity by two orders of magnitude. A high efficiency discrete infrared LED–photodiode pair is demonstrated to provide measurements of corona currents between 0.2 and 20 μA using a second LED–photodiode pair for analog linearity compensation. The inherent simplicity is well suited to new applications of ion emission in propulsion and weather modification.

© 2023 Author(s). All article content, except where otherwise noted, is licensed under a Creative Commons Attribution (CC BY) license (<http://creativecommons.org/licenses/by/4.0/>). <https://doi.org/10.1063/5.0170176>

I. INTRODUCTION

Discharge from high voltage electrodes provides a convenient source of unipolar ions for charging^{1,2} propulsion³ and atmospheric² experiments. Although atmospheric discharge currents near earth potential can be measured straightforwardly,⁴ determining the current flowing from an ionizer requires a “high side” measurement at what may be a considerable operating potential of the electrode. This is typically achieved by floating the measuring electronics at the high potential and returning the signal through optical isolation^{5–8} because of voltage stress limitations on integrated circuits. Such methods usually also require an isolated supply to power the current measurement circuit,⁹ which in our application of monitoring ion dispersal from an aircraft¹⁰ added complexity and volume in an already physically constrained system. Using a light-emitting diode (LED) to passively sense and signal the current offers a simpler alternative for unipolar systems, with negligible effect on operation as the LED forward voltage ($\sim 2\text{ V}$) is small in comparison with the electrode voltage. Such an approach has been used with a photomultiplier,¹¹ but a minimum current of 80 μA was required to operate the linearizing circuitry using specific hybrid parts with limited

voltage isolation. Currents associated with an atmospheric ionizer are typically much smaller ($\sim 1\text{ }\mu\text{A}$). Here, a method is described that is based on an efficient infrared LED to sense small corona currents passively for monitoring ionizer operation.

II. DESIGN CONSIDERATIONS

A. Component characterization

Optocoupler devices are generally housed in an integrated package, containing a photoemitter and photodetector. Standard LED–phototransistor optocouplers (e.g., the 4N35) intended for digital use, operate with LED currents several orders of magnitude greater than $\sim 1\text{ }\mu\text{A}$ envisaged for corona current measurement. The IL300 analog (LED–photodiode) optocoupler is also unsatisfactory at these relatively small LED currents.¹¹ Although using a separate LED and a spectrally matched photodiode is less convenient practically, it allows the selection of a high efficiency LED able to operate at the low current required and removes the isolation voltage limitations of integrated optocoupler packages.

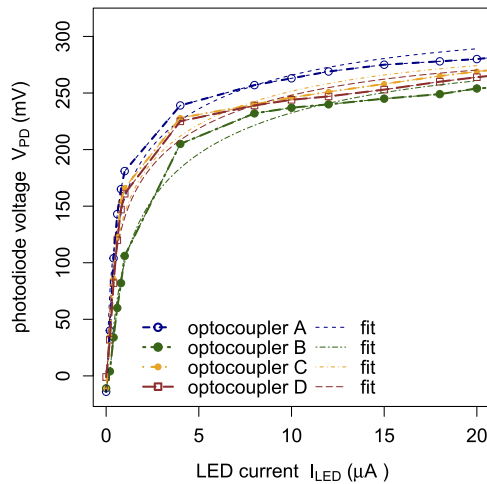


FIG. 1. Current-voltage characteristics of four optocoupler pairs (A, B, C, and D), each consisting of a OSI3NA5111A LED and SFH213 photodiode facing each other in a light-tight tube. The LED currents were generated by an opamp (LM358) constant current source, and the photodiode open circuit voltage (points) were determined by a digital voltmeter with a 1 MΩ input resistance. Thick dashed lines join the points; thin dashed lines are calculated fits to Eq. (3), obtained by non-linear least-squares optimization.

A discrete LED-photodiode combination has therefore been investigated for its response to the small unipolar input currents expected. The OSI3NA5111A LED and SFH213 photodiode were chosen for this based on their efficiency and sensitivity, respectively. Both are 5 mm diameter through-hole parts, operating at 850 nm. Their lower halves were each painted with black nail varnish to exclude external light and held facing each other – but not touching – within black heat-shrink tubing. An opamp constant current source was used to generate a range of LED forward currents with the photodiode open circuit voltages V_{PD} measured. Figure 1 shows responses obtained for four different LED-photodiode pairs, indicating an initially rapid increase in V_{PD} with I_{LED} from about $I_{LED} = 0.2 \mu\text{A}$, followed by a more gradual increase for $I_{LED} \gg 1 \mu\text{A}$. The four optocoupler pairs show broadly similar response but differ in detail.

As the LED and photodiode are physically separate parts, the measured photodiode voltage and LED forward current are associated with two semiconductor junctions. However, their combined response in Fig. 1 is reminiscent of a single diode.¹² The classical form of this is

$$V_f = nV_T \ln \left(\frac{I_f}{I_s} + 1 \right) \quad (1)$$

for I_f the diode's forward current, I_s the saturation current, n the ideality factor, V_f the forward voltage, and V_T the thermal voltage $\approx \frac{kT}{e}$. If the coupling between the two parts is regarded as, first, through the LED having an optical output proportional to its forward current and, second, through the photodiode having a linear response to light received,¹³ Eq. (1) can be approximated by

$$V_{PD} \propto \ln \left(1 + \frac{\eta I_{LED}}{I_{sPD}} \right), \quad (2)$$

where I_{sPD} is the saturation current of the photodiode and η is the coupling efficiency factor between optical emission of the LED and the generated photodiode current. As anticipated from these theoretical considerations, Eq. (2) provides an approximate fit to the measured data, but it can be improved by including an Ohmic term as

$$V_{PD} = \eta I_{LED} R_0 + nV_T \ln \left(1 + \frac{\eta I_{LED}}{I_{sPD}} \right). \quad (3)$$

Fits to the data derived using (3) with a least-squares procedure are also shown in Fig. 1, assuming $V_T = 26 \text{ mV}$. Derived values of n lie between two and three.

B. Signal processing

Because of the abrupt transition in the response apparent in Fig. 1, some compensation for the non-linear sensitivity is desirable. (Experiments with the optocouplers at 17 °C and −21 °C showed that the temperature variation was negligible in comparison). Reviewing Fig. 1, optocouplers C and D show the closest comparability, which offers the possibility of using one optocoupler to compensate for the variations in another. Such a compensation scheme has been implemented with analog electronics, using a differential amplifier to compare the photodiode voltage from one optocoupler with that from a second optocoupler, the LED current for which is continuously adjusted by feedback. When the photodiode voltages are equal, the second (compensating) optocoupler's LED current provides an estimate of the current flowing in the first (sensing) optocoupler's LED and ultimately the corona current. Depending on the closeness of the device matching and coupling efficiencies, this compensates for the non-linearity. Figure 2 summarizes the approach. In detail, the differential amplifier was constructed for minimal loading of the photodiodes using 10 MΩ input resistors with unity gain (and 1 nF across the feedback resistor for stability) from one stage of a low bias current LMC6042 opamp; the second opamp in the package was used to construct a feedback current source with a single 100 kΩ resistor. A simple opamp current source is possible because LED2

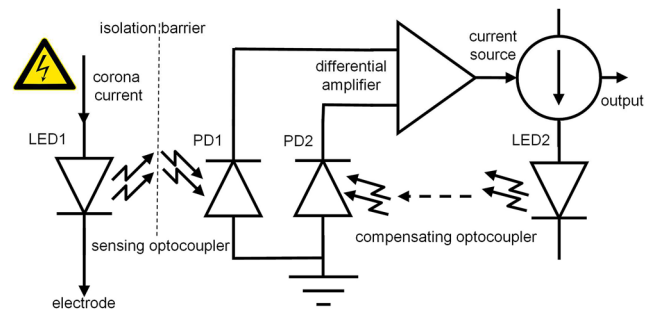


FIG. 2. Signal processing and non-linearity compensation. LED1 and PD1 form an optocoupler, generating a voltage at PD1 proportional to the current flowing through LED1. A second photodiode (PD2) voltage is compared with that from PD1 by a differential amplifier, which controls the current source driving LED2, illuminating PD2. Feedback adjusts the LED2 current to cause the PD2 voltage to equal that of PD1. The LED2 control voltage provides a compensated determination of the LED1 current, V_o .

presents a floating load, and the LMC6042 permits single supply operation.

III. RESULTS

A. Current retrieval

Figure 3 shows the response of one optocoupler to a range of LED1 currents (open circles), and, additionally, the simultaneous output V_o of the Fig. 2 circuit to the same input currents by using a second optocoupler for compensation. This was originally intended to reduce thermal effects in an aircraft application, but more importantly, it also increases the sensitivity, which would otherwise be close to the analog to digital converter resolution of 1 mV. Overall, this gives an output change approximately double that of the single optocoupler over the range 0.2 to 20 μA with the step in the LED currents evident in Fig. 1 reduced. Further processing is applied to improve the current retrieval's accuracy.

Accurate retrieval of the LED1 current from V_o requires inversion of the observed response. This is achieved graphically by fitting a curve to the data to calculate the LED1 current at the voltage required. Following Fig. 1, Eq. (3) also provides a suitable fit to the compensated response and yields the dashed line in Fig. 3 with two characterizing coefficients. A disadvantage is that Eq. (3) cannot be inverted analytically. Instead, I_{LED1} is found numerically by solving $f(I_{LED1}) = 0$ for an observed output voltage V_o using the Newton-Raphson method, where

$$f(I_{LED1}) = \eta I_{LED1} R_0 + n V_T \ln \left(1 + \frac{\eta I_{LED1}}{I_{SPD}} \right) - V_o. \quad (4)$$

A starting value of 0.2 μA for I_{LED1} leads to the solution in about five iterations using a convergence criterion of 10^{-4} μA between successive values.

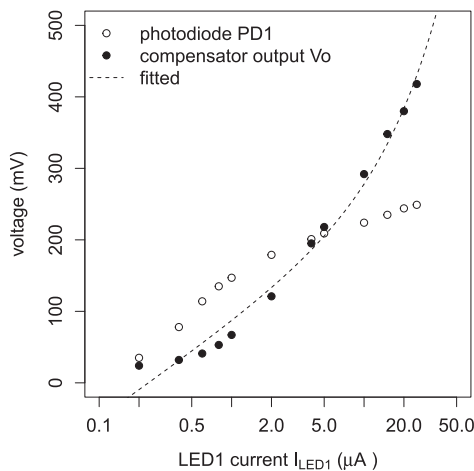


FIG. 3. Raw optocoupler response (dashed line) of the photodiode PD1 voltage to the imposed LED1 current (open circles) with the simultaneous output voltage (solid circles) from the compensated Fig. 2 system. The dashed line shows Eq. (3) fitted to the compensated voltage data (derived coefficients: $\eta R_0 = 5482.4 \, \Omega$ and $\eta/I_{SPD} = 6.011 \times 10^{-7} \, \text{A}^{-1}$ for fixed $V_T = 26 \, \text{mV}$ and $n = 3$).

B. Ionizer application

The intended use of the LED optocoupler to sense corona currents was evaluated by combining it with a resistor-based measurement of the same current, at the high voltage generated by the ionizer. A stand-alone test system was implemented to avoid risk to a logging computer from the high voltages present. Figure 4 shows the arrangement using the optocouplers of Fig. 3.

The current from a negative ionizer (Amazon type B01G1DA19O) was passed through a sensing resistor and a LED current sensor to a brush electrode emitter. The voltage developed across the resistor was measured using a battery-powered differential amplifier (constructed in a standard way from 680 k Ω 0.1% resistors with an OP97 opamp chosen for common mode rejection), sampled by the Analog to Digital Converter (ADC) of a 12F675 microcontroller. The microcontroller was programmed to average at 0.5 s intervals the differential amplifier voltage, a 2.5 V reference, and the mid-point of the power supply from 16 samples in each case. These values were sent as a serial data packet through an optical isolator to an Arduino Uno development board with an SD card. After receiving a data packet, the Arduino Uno sampled the compensated LED voltage from an analog input, writing the combined data received to the SD card.

Electrical noise produced by the ionizer necessitated a decoupling capacitor from the high voltage part of the circuit to earth, and a slow data rate (300 baud) for the serial transfer was required for reliability. Furthermore, it was found necessary to ensure that there were no sharp bends in the high voltage con-

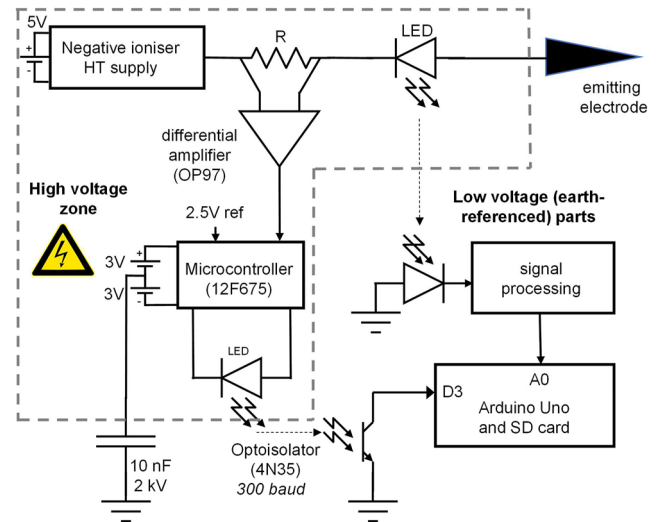


FIG. 4. Block diagram of the test system. A negative ionizer (with a high tension, HT supply) is connected to a brush electrode emitter through a current sensing series resistor R (10 k Ω) and the LED of an optocoupler. The resistor voltage is monitored using a battery-powered differential amplifier and microcontroller. Samples of the resistor voltage at 0.5 Hz together with samples of a 2.5 V reference are sent as serial data through an optoisolator to an Arduino Uno. Whenever a data packet is received at its digital input D3, the Arduino Uno also samples the optocoupler photodiode at analog input A0. All values are timestamped and written to the SD card.

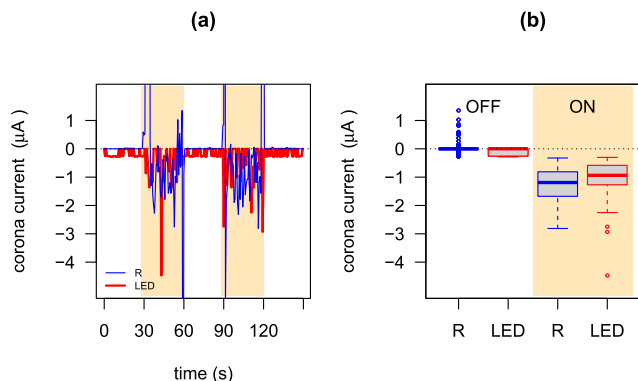


FIG. 5. (a) Time series of corona currents with the ionizer switched on (straw background) and off (white background), measured with the Fig. 4 system using the current-sense resistor (thin blue line, R) and LED sensor (thick red line, LED) methods. (b) shows the same data grouped into boxplots for the ionizer switched off and on (on currents $< -0.3 \mu\text{A}$). (Boxplots show, in each case, the median as a solid line, the inter-quartile range IQR as the size of the box, and whiskers to 1.5 IQR¹⁴).

nections between the resistor and LED to prevent corona current losses.

The ionizer was pulsed on and off manually in bursts of ~ 30 s with the data recorded by the Arduino on the SD card. The micro-controller ADC values were scaled against the 2.5 V reference and converted to bipolar voltages. The associated photodiode voltage samples were converted to the LED current using Eq. (4), applying the Newton–Raphson method on each value. Figure 5 compares current measurements from the two methods, LED and resistor (R). Figure 5(a) shows time series with the ionizer off initially and then switched on and off for 30 s twice. Under the off condition, the LED-derived current fluctuates between 0 and $-0.3 \mu\text{A}$. Under the on condition, the traces show switching transients and noise, but the values from the two methods are weakly positively correlated, suggesting a common source. Selecting the inner part of the ionizer-on data to avoid the transients for currents exceeding the LED offset ($-0.3 \mu\text{A}$), the median ionizer-on currents are during the first pulse $-1.1 \mu\text{A}$ (LED) and $-1.3 \mu\text{A}$ (R) from 13 values and during the second pulse $-0.93 \mu\text{A}$ (LED) and $-0.97 \mu\text{A}$ (R) from 15 values. Figure 5(b) presents the on and off currents as boxplots. As for the separate pulses, the median currents measured separately by the resistor and LED methods appear similar although data limitations could cause spurious concordance.

IV. CONCLUSION

This work demonstrates that a high efficiency LED can provide a passive method of fully isolated low current measurement suitable for corona current applications. Different physical forms of LEDs may offer more compact arrangements or permit larger isolation voltages, but it seems unlikely that the simplicity of the unpowered isolated sensor can be improved.

ACKNOWLEDGMENTS

This material is based on work supported by the National Center of Meteorology, Abu Dhabi, UAE, under the UAE Research Program for Rain Enhancement Science (UAEREP). Ahmad Al Kamali helped with testing of prototypes. We thank Ralph Lorenz and an anonymous reviewer for their helpful comments.

AUTHOR DECLARATIONS

Conflict of Interest

The authors have no conflicts to disclose.

Author Contributions

R. Giles Harrison: Conceptualization (lead); Data curation (lead); Funding acquisition (equal); Software (lead); Writing – original draft (lead). **Veronica Escobar-Ruiz:** Investigation (equal); Resources (equal); Writing – review & editing (equal). **Keri A. Nicoll:** Funding acquisition (equal); Investigation (equal); Supervision (equal); Writing – review & editing (equal). **Maarten H. P. Ambaum:** Formal analysis (equal); Funding acquisition (equal); Writing – review & editing (equal).

DATA AVAILABILITY

The data that support the findings of this study are available from the corresponding author upon reasonable request.

REFERENCES

- W. Balachandran, A. Jaworek, A. Krupa, J. Kulon, and M. Lackowski, "Efficiency of smoke removal by charged water droplets," *J. Electrostat.* **58**(3–4), 209 (2003).
- X. Yan and Y. Jiang, "Numerical evaluation of the fog collection potential of electrostatically enhanced fog collector," *Atmos. Res.* **248**, 105251 (2021).
- H. Xu, Y. He, K. L. Strobel, C. K. Gilmore, S. P. Kelley, C. C. Hennick, T. Sebastian, M. R. Woolston, D. J. Perreault, and S. R. H. Barrett, "Flight of an aeroplane with solid-state propulsion," *Nature* **563**(7732), 532 (2018).
- R. D. Lorenz, L. D. V. Neakrase, J. P. Anderson, R. G. Harrison, and K. A. Nicoll, "Point discharge current measurements beneath dust devils," *J. Atmos. Sol.-Terr. Phys.* **55**, 150–151 (2016).
- P. Wang and G. Zhang, "The measurement method for corona discharge current under high-voltage environment," *IEEE Trans. Instrum. Meas.* **57**(8), 1786 (2008).
- K. L. Aplin, K. L. Smith, J. G. Firth, B. J. Kent, M. S. Alexander, and J. P. W. Stark, "Inexpensive optically isolated nanoammeter for use with micro-Newton electric propulsion technology," *J. Propul. Power* **24**(4), 892 (2008).
- A. Band and J. Unguris, "Optically isolated current-to-voltage converter for an electron optics system," *Rev. Sci. Instrum.* **68**(1), 250 (1997).
- R. G. Harrison, "A wide-range electrometer voltmeter for atmospheric measurements in thunderstorms and disturbed meteorological conditions," *Rev. Sci. Instrum.* **73**(2), 482 (2002).
- R. G. Harrison, K. A. Nicoll, D. J. Tilley, G. J. Marlton, S. Chindea, G. P. Dingley, P. Iravani, D. J. Cleaver, J. L. Du Bois, and D. Brus, "Demonstration of a remotely piloted atmospheric measurement and charge release platform for geoeengineering," *J. Atmos. and Oceanic Technol.* **38**(1), 63–75 (2021).

¹⁰R. G. Harrison, K. A. Nicoll, G. J. Marlton, D. J. Tilley, and P. Iravani, “Ionic charge emission into fog from a remotely piloted aircraft,” *Geophys. Res. Lett.* **49**(19), e2022GL099827, <https://doi.org/10.1029/2022gl099827> (2022).

¹¹S. Argirò, D. V. Camin, M. Destro, and C. K. Guérard, “Monitoring DC anode current of a grounded-cathode photomultiplier tube,” *Nucl. Instrum. Methods Phys. Res., Sect. A* **435**(3), 484 (1999).

¹²W. Shockley, “The theory of p - n junctions in semiconductors and p - n junction transistors,” *Bell Syst. Tech. J.* **28**(3), 435 (1949).

¹³W. Shockley and H. J. Queisser, “Detailed balance limit of efficiency of p - n junction solar cells,” *J. Appl. Phys.* **32**(3), 510 (1961).

¹⁴R Core Team, “R: A language and environment for statistical computing,” *R Foundation for Statistical Computing*, 2021.